

# Patterns of Spontaneous Purkinje Cell Complex Spike Activity in the Awake Rat

Eric J. Lang,<sup>1</sup> Izumi Sugihara,<sup>2</sup> John P. Welsh,<sup>1</sup> and Rodolfo Llinás<sup>1</sup>

<sup>1</sup>Department of Physiology and Neuroscience, New York University Medical Center, New York, New York 10016, and

<sup>2</sup>Department of Physiology, Tokyo Medical and Dental University School of Medicine, 1-5-45 Yushima, Bunkyo-ku, Tokyo 113–8519, Japan

The olivocerebellar system is known to generate periodic synchronous discharges that result in synchronous (to within 1 msec) climbing fiber activation of Purkinje cells (complex spikes) organized in parasagittally oriented strips. These results have been obtained primarily in anesthetized animals, and so the question remains whether the olivocerebellar system generates such patterns in the awake animal. To this end, multiple electrode recordings of crus 2a complex spike activity were obtained in awake rats conditioned to execute tongue movements in response to a tone. After removal of all movement- and tone-related activity, the remaining data were examined to characterize spontaneous complex spike activity in the alert animal. Spontaneous complex spikes occurred at an average firing rate of 1 Hz and a clear  $\approx 10$  Hz rhythmicity. Analysis of the autocorrelograms using a rhythm index indicated that the

large majority of Purkinje cells displayed rhythmicity, similar to that in the anesthetized preparation. In addition, the patterns of synchronous complex spike activity were also similar to those observed in the anesthetized preparation (i.e., simultaneous activity was found predominantly among Purkinje cells located within the same parasagittally oriented strip of cortex). The results provide unequivocal evidence that the olivocerebellar system is capable of generating periodic patterns of synchronous activity in the awake animal. These findings support the extrapolation of previous results obtained in the anesthetized preparation to the waking state and are consistent with the timing hypothesis concerning the role of the olivocerebellar system in motor coordination.

**Key words:** olivocerebellar; synchrony; oscillation; rhythmicity; inferior olive; climbing fiber

The olivocerebellar system constitutes one of the two major afferent systems to the cerebellum, and its activity is central to motor coordination because lesions of the inferior olive are followed by severe motor disturbances, similar to those resulting from cerebellar damage (Soechting et al., 1976). Yet the exact contribution of olivocerebellar activity to cerebellar functioning continues to be much debated (for review, see Simpson et al., 1996). The enigmatic status of the olivocerebellar system is probably in large measure caused by the rather unusual characteristics of its activity. Indeed it has been argued that because of its low average single-cell firing rate of  $\approx 1$  Hz and maximum rate of  $\approx 10$  Hz, the olivocerebellar system cannot produce significant changes in cerebellar output on its own (Keating and Thach, 1995). However, an alternative, suggested by its physiological and anatomical organization, is that the olivocerebellar system may alter cerebellar output by the temporal binding property generated by the synchronous activation of sets of neuronal ensembles (Llinás and Sasaki, 1989).

The ability of the olivocerebellar system to generate ensemble synchronous activity has been extensively documented using multiple electrode recording of complex spikes (CSs) from Purkinje cells in anesthetized animals (Bell and Kawasaki, 1972; Llinás

and Sasaki, 1989; Sasaki et al., 1989; Sugihara et al., 1993; Wylie et al., 1995; Lang et al., 1996, 1997). At the level of the cerebellar cortex, these patterns most often take the form of simultaneous (to within 1 msec) CSs in parasagittally oriented strips of Purkinje cells (Llinás and Sasaki, 1989; Sasaki et al., 1989; Sugihara et al., 1993). The simultaneity of CS activity has been ascribed to the electrotonic coupling of inferior olivary neurons via gap junctions located mainly in structures known as glomeruli (Llinás et al., 1974; Sotelo et al., 1974; Llinás and Yarom, 1981a) and a matching of axonal conduction velocity to climbing fiber length (Sugihara et al., 1993). However, these patterns are not unchangeable entities fixed by the anatomical connectivity of the system. Rather, the specific spatial distribution of synchronous CS activity is determined primarily by the ongoing activity of the GABAergic cerebellar nucleo-olivary pathway, which provides a major synaptic input to the olivary glomeruli (de Zeeuw et al., 1989) and can produce momentary functional decoupling of inferior olive (IO) neurons (Lang et al., 1996). Thus, this parasagittal banding pattern reflects a particular functional state of the olivocerebellar system, whereas other functional states would be represented by other such patterns. Indeed, distinct patterns of synchronous CS activity occur in relation to given movements (Welsh et al., 1995a).

Olivocerebellar activity is also characterized by an 8–12 Hz rhythmicity. Using *in vitro* techniques or *in vivo* anesthetized or decerebrated preparations, this rhythmicity has been amply documented in a number of species (Belcari et al., 1977; Llinás and Yarom, 1981a,b, 1986; Bloedel and Ebner, 1984; Benardo and Foster, 1986; Llinás and Sasaki, 1989; Sasaki et al., 1989; Lampi and Yarom, 1993, 1997; Sugihara et al., 1995; Wylie et al., 1995;

Received Sept. 22, 1998; revised Jan. 12, 1999; accepted Jan. 17, 1999.

This work was supported by the National Institutes of Health/National Institute of Neurological Diseases and Stroke (NS13742, NS37028, NS31224), the Office of Naval Research (N00014-93-1-0225), and the National Science Foundation (IBN-9808353).

Correspondence should be addressed to Dr. E. J. Lang or Dr. R. Llinás, Department of Physiology and Neuroscience, New York University Medical Center, 550 First Avenue, New York, NY 10016.

Copyright © 1999 Society for Neuroscience 0270-6474/99/192728-12\$05.00/0

Lang et al., 1996, 1997) and may become particularly pronounced and lead to phase-locked motor activity with tremorigenic drugs such as harmaline (de Montigny and Lamarre, 1973; Llinás and Volkind, 1973).

Taken together these results provide significant evidence that the olivocerebellar system generates periodic synchronous discharges and support for the hypothesis that it functions as an internal clock for organizing motor sequences (Llinás, 1991). Nevertheless, because these studies were performed in anesthetized animals or *in vitro* preparations, their relevance to the normal physiological activity of the olivocerebellar system may be questioned, and so the extent to which the activity observed under the different anesthetic states reflects the normal spontaneous activity patterns in the awake animal must be determined.

Spontaneous CS activity has in fact been reported to display an  $\approx 10$  rhythmicity in awake frogs (Rushmer and Woodward, 1971) and guinea pigs (Bell and Kawasaki, 1972); however, these initial reports did not quantify its strength or prevalence. Moreover, whereas studies in behaving rodents have demonstrated CS rhythmicity (Welsh et al., 1995a,b), those in primates have produced mixed results, with some investigators finding rhythmic CS activity (Pellerin et al., 1997) and others not (Keating and Thach, 1995). Thus, the presence of rhythmic CS activity in the awake animal remains somewhat controversial.

Although CS synchrony in awake animals has been previously reported (Bell and Kawasaki, 1972), recordings were obtained from only a limited number ( $n = 5$ ) of closely spaced cell pairs, preventing any conclusions about the spatial extent of synchronous activity from being drawn. More recently, multiple electrode recordings have been used to determine the movement-related patterns of synchronous CS activity (Welsh et al., 1995a). In this study, the patterns of synchronous CS activity differed significantly from the parasagittal banding patterns observed in anesthetized preparations (Welsh et al., 1995a). In particular, movement-related synchronization of CS activity was found between Purkinje cells located in different parasagittal planes. This difference may have stemmed from the fact that the functional states of the olivocerebellar and cerebellar nucleo-olivary systems are very different in the anesthetized and awake animals, thus limiting the conclusions to be drawn from studies in anesthetized preparations concerning the spatial distribution of spontaneous synchronous activity. Alternatively, this difference may have been caused by the generation of specific movement-related patterns. To test these alternatives, a quantitative description of the spontaneous patterns of synchronous CS activity in the awake animal is needed. And so, to determine the rhythmicity and spatial patterns of synchrony inherent in spontaneous CS activity, we have obtained multiple electrode recordings of spontaneous (i.e., non-movement related) CS activity in awake rats. The results indicate that in the waking state, the olivocerebellar system generates spontaneous patterns of rhythmic and synchronous CS activity similar to what has been described in the anesthetized animal.

## MATERIALS AND METHODS

### *Surgical and recording procedures*

Adult Sprague Dawley rats (225–300 gm) were used in all experiments. These animals had been previously trained to perform a conditioned tongue movement task in which a tone elicited a series of licks (Welsh et al., 1995a). On the day of the recording, they were anesthetized with an injection of ketamine (100 mg/kg, i.p.) and implanted with an array of microelectrodes for recording CS activity from crus 2a of the cerebellar cortex. The implantation technique has been described previously

(Sasaki et al., 1989; Sugihara et al., 1993). In brief, a craniotomy was performed to expose the crus 2 region of the left cerebellar hemisphere. After removal of the dura mater, a silicon rubber-coated titanium electron microscope grid was cemented in place over crus 2a. Glass microelectrodes filled with a 1:1 solution of glycerol and saline were individually inserted to a depth of  $\approx 100$   $\mu$ m where CS activity from individual Purkinje cells could be recorded extracellularly. Interelectrode spacing was 250  $\mu$ m. After implantation of the electrode array, the animals were allowed to recover from the anesthesia.

Spontaneous CS activity described in the present report was obtained during two types of conditions. First, recordings were obtained from a 10–20 min period just before the beginning of conditioned movement sessions during which the animals were alert but relatively inactive. Second, CS activity was analyzed from the nonmovement periods during the conditioned movement sessions. In these sessions, the animal's head was immobilized, and movements of the tongue and jaw were monitored with infrared photoemitter-detector devices. The conditioned movement sessions typically lasted  $\approx 4$  hr and contained  $\approx 500$  trials that were initiated by a tone that occurred once every 30 sec on average. The tone was followed by a series of 6–7 Hz licking movements that typically lasted  $\approx 0.5$  sec. To exclude movement-related and tone-related CS activity, the data from 1 sec before until 5 sec after the tone onset were eliminated, and only the activity from the remaining 24 sec between trials was analyzed. In addition, because the animals made occasional tongue and mouth movements during the intertrial periods, CS activity from  $\pm 200$  msec surrounding such movements was eliminated.

For comparative purposes, data from multiple electrode experiments in anesthetized rats were analyzed. In these experiments, the animals were anesthetized with an initial injection of ketamine (100 mg/kg, i.p.), xylazine (8 mg/kg, i.p.), and atropine (0.4 mg/kg, i.p.). The heart rate was monitored, and supplemental doses of anesthetic were given to maintain a deep anesthetic level. The surgical procedures were similar to those described above for the awake animals and have been previously described in detail (Sasaki et al., 1989; Lang et al., 1996). Recording sessions typically lasted 15–30 min.

### *Data analysis*

**Analysis of CS synchrony.** Here, as previously, we define CSs that occur in different Purkinje cells as being synchronous when their onsets occur within 1 msec of each other. The degree of synchronous activity displayed by different cell pairs was quantified by calculating  $C(0)$ , the zero-time cross-correlation coefficient, using a time bin of 1 msec, as described previously (Sasaki et al., 1989; Lang et al., 1996). The term “synchronicity” is used to refer to the spatial distribution of synchronous activity and was quantified by calculating  $C(0)$  for all possible cell pairs and then plotting the average value of  $C(0)$  as a function of the medio-lateral separation distance between the cells within a pair.

**Analysis of CS rhythmicity.** Autocorrelation histograms were constructed from the CS activity of individual Purkinje cells using time bins of 5 or 10 msec. The oscillation frequency was taken as the reciprocal of the latency of the first peak in the autocorrelogram. The strength of the oscillation was quantified with a rhythm index (RI) calculated in a similar manner to that described previously (Sugihara et al., 1995; Lang et al., 1997). In brief, the autocorrelation coefficients of all peaks and valleys in the autocorrelogram that (1) were significantly different from the baseline and (2) occurred at specific latencies with regard to the initial peak were summed. Peaks and valleys were considered significant if they were  $>1$  SD above or below the average level, respectively. The SD was determined using bins at time lags of 1.5–2 sec where there was no evident periodic activity. The average level was measured from bins of time lags of 50 msec to 1 sec. In the autocorrelograms that had no significant peaks and valleys, a value of zero was given to the RI, and the activity was considered nonoscillatory. In these cases, or when the RI was less than an empirically determined value of 0.01, the oscillation frequency was not determined. The latter cases were excluded because the autocorrelograms of such cells ( $0 < RI < 0.01$ ) displayed only weak rhythmicity with peaks that were very close to the baseline activity (see Fig. 5A), making unambiguous determination of the primary peak, and therefore the oscillation frequency, difficult.

### *Runs test to detect systematic variation over time*

Runs tests were used to determine any trend over time in the values of the parameters used to measure CS rhythmicity and synchrony. First, the recording sessions were divided into 25 min segments, and the values of the parameters were calculated for each segment. A runs test was then

performed on the sequence of values obtained for each parameter. The runs test determines whether the successive values in the time sequence are correlated or whether they vary about the median as expected by chance. First, the number of times that the time sequence crosses its median value is calculated. The number of runs is then equal to the number of crossings plus one. The observed number of runs ( $R_o$ ) can then be compared with the expected number ( $R_e$ ) and a  $z$  value determined as  $(R_o - R_e)/(SD)$  where  $R_e \approx (n/2) + 1$ , the  $SD \approx [(n - 1)/4]^{1/2}$ , and  $n$  is the number of observations in the time sequence (Wonnacott and Wonnacott, 1977). Thus, a significant trend over time in the data is indicated by  $z$  values more negative than  $-1.65$ , which corresponds to a  $p$  value of 0.05 that  $R_o$  would be observed by chance.

## RESULTS

### Database

The present results were obtained from animals ( $n = 11$ ) that were operantly conditioned to perform tongue movements in response to a tone. The movement-related CS activity recorded from these animals has been previously reported (Welsh et al., 1995a). Here we describe the patterns of spontaneous CS activity recorded while the animals were not making any overt movements. This activity was recorded either from an  $\approx 15$ –20 min period before the actual conditioning session started, during which the animal was sitting quietly ( $n = 2$ ), or from the intertrial periods of the conditioning session when no tongue or mouth movements were occurring ( $n = 9$ ). In total, CS activity was recorded from 282 crus 2a Purkinje cells (range, 16–33 cells per animal). The average CS firing rate for these cells was  $1.01 \pm 0.70$  Hz (mean  $\pm$  SD), similar to previous reports in awake animals (Mano, 1970; Hobson and McCarley, 1972; Armstrong and Rawson, 1979).

For comparative purposes, the data from seven multiple electrode experiments ( $n = 257$  Purkinje cells) in which the animals were anesthetized with ketamine–xylazine anesthesia is described. A similar, but somewhat higher average CS firing rate ( $1.52 \pm 0.89$  Hz) was observed in these experiments.

### CS synchrony in the awake rodent

Spontaneous CS activity in the awake animal showed a similar spatial organization to that observed in the anesthetized preparation. There were generally much higher levels of synchronous CS activity among neighboring Purkinje cells than among widely separated Purkinje cells. In particular, the degree of synchronous CS activity dropped off rapidly as the mediolateral separation between the Purkinje cells increased, similar to what was observed in the anesthetized preparation (Llinás and Sasaki, 1989; Sasaki et al., 1989). Thus, the spatial organization of CS synchrony displayed a rostrocaudal preference, with Purkinje cells within the same parasagittal strip of cortex having the highest levels of synchrony. Examples of the spatial organization of CS synchrony from an experiment in which 29 Purkinje cells were simultaneously recorded are shown in Figure 1*A*. The relative positions of the Purkinje cells are represented by the positions of the circles in the plots and correspond to the electrodes of the array shown in Figure 1*B*. The degree of synchronous CS activity between a master cell ( $M$ ) and each of the 28 other Purkinje cells was determined by calculating  $C(0)$  for each cell pair and is indicated by the areas of the corresponding circles. In these and subsequent plots, synchronous is defined as two CSs whose onsets are within 1 msec of each other. Note how the pattern of synchronization shifts according to which cell is chosen as the master cell, such that Purkinje cells showing the highest levels of synchronization occur within the same parasagittal strip of cortex as the master cell (Fig. 1, compare  $A_1$ ,  $A_2$ ).

The temporal precision of this synchrony is shown by the cross-correlograms of Figure 1*C*. The cross-correlogram on the right shows the relationship of activity between cell  $M$  of Figure 1*A*<sub>2</sub> and the cell located 500  $\mu$ m rostral ( $b$ ). Although there was a general increase in the correlation for  $\pm 20$  msec, by far the strongest correlation occurred at a time lag of 0 msec. Thus, the CS discharges of these cells had a strong tendency to be synchronized to within 1 msec. In contrast, the cross-correlogram on the left shows the relationship of activity between cell  $M$  and the cell located 500  $\mu$ m lateral ( $a$ ). There is almost no synchronization of the CS activity of these two Purkinje cells, as indicated by the flatness of the correlogram.

The spatial distribution of CS synchrony relative to the master cell was similar regardless of the choice of the master cell. This was demonstrated by calculating  $C(0)$  for all possible cell pairs and then plotting the average  $C(0)$  value as a function of the mediolateral separation distance between the cells (Fig. 2). The plot of Figure 2*A*<sub>b</sub> corresponds to the experiment shown in Figure 1. As was suggested by the examples shown in Figure 1, the highest level of synchronization on average occurred among Purkinje cells located within the same parasagittal plane (0  $\mu$ m mediolateral separation distance). At a separation distance of 250  $\mu$ m there was still a significant degree of synchronization, but at distances of 500  $\mu$ m and greater virtually no synchronization occurred.

A similar distribution of CS synchrony was observed in most of the 11 experiments performed in nonanesthetized animals. Plots of average CS synchrony as a function of mediolateral separation distance are shown for each of the experiments in Figure 2*A*. In all cases, the average CS synchrony was significantly ( $p < 0.02$ ; two-sided  $t$  test) higher for smaller separation distances ( $\leq 500$   $\mu$ m;  $0.018 \pm 0.030$ ;  $n = 33$ ) than for larger separation distances ( $> 500$   $\mu$ m;  $0.0045 \pm 0.0075$ ;  $n = 67$ ). In the large of majority experiments (9 of 11), the highest degree of synchronization was found among Purkinje cells within the same parasagittal plane (Fig. 2*Aa–e,g*) or within 250  $\mu$ m of each other (Fig. 2*Af,h,j*). The synchrony plots from these experiments were normalized to the synchrony value at 0  $\mu$ m separation distance (Fig. 2*B*), and the average normalized distribution of synchrony was determined (Fig. 2*C*). The shape of this curve demonstrates that the CS activity of Purkinje cells separated by  $< 500$   $\mu$ m in the mediolateral direction was significantly more synchronized than that of Purkinje cells that were more greatly separated. In sum, the spatial distribution of synchrony of spontaneous CS activity in nonanesthetized animals displayed a parasagittal banding pattern.

### Temporal stability of banding structure

The above results demonstrated the presence of a parasagittal banding organization to CS synchrony in the waking state. We next investigated the stability of this banding pattern over time by dividing the  $\approx 4$  hr recording sessions into successive 25 min periods and determining the spatial distribution of CS synchrony for each period. In each experiment ( $n = 8$ ), it was found that while the average level of CS synchrony did vary between the successive periods, the overall spatial pattern remained constant. The results from one experiment are plotted in Figure 3*A*, in which the distribution of CS synchrony for nine successive 25 min periods is shown. Note that despite some fluctuation in the average level of CS synchrony at each separation distance, the shapes of the curves are quite similar. Even in experiments where there was some variation from the typical synchrony distribution

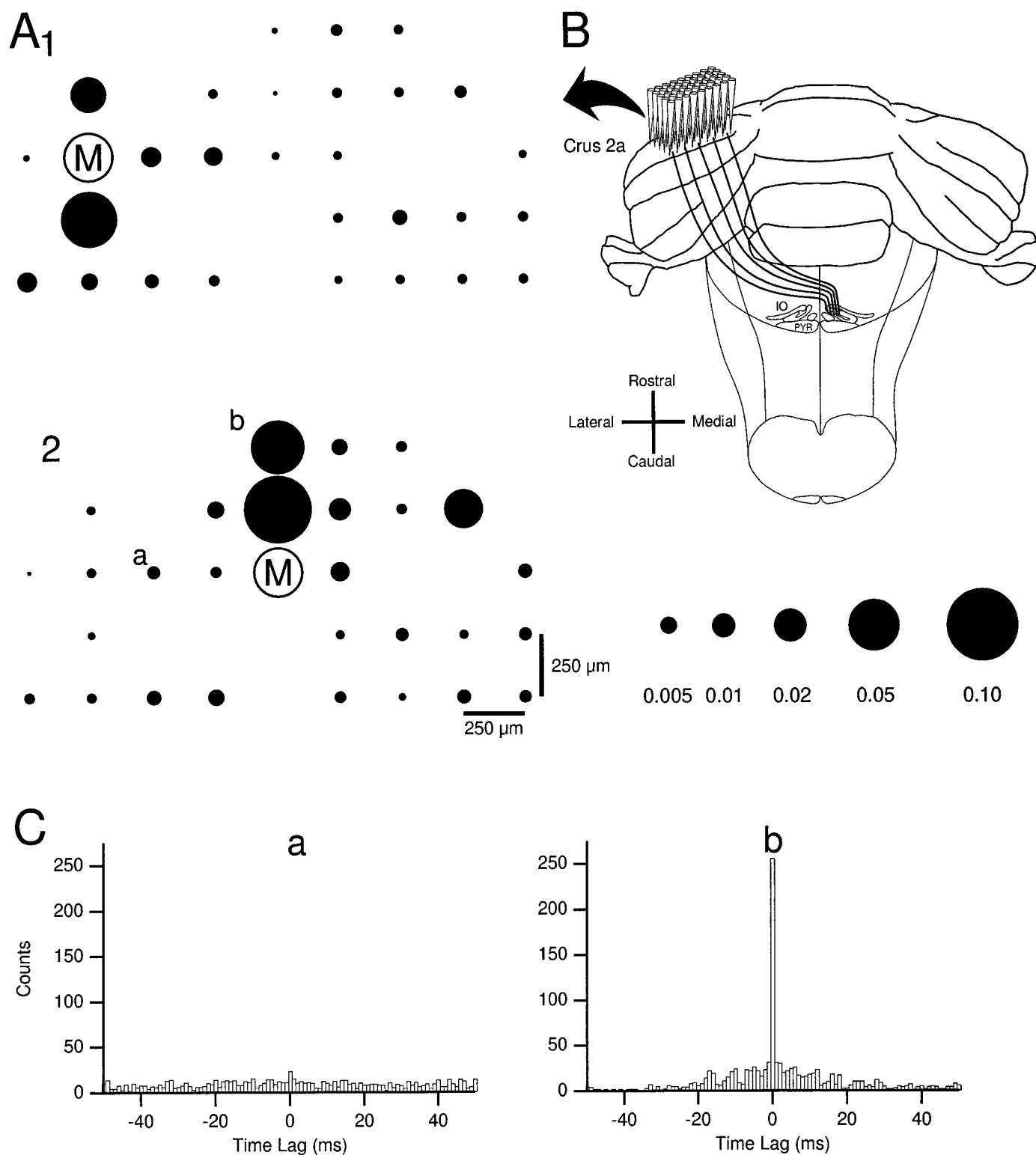


**Figure 1.** CS synchrony in a nonanesthetized rat. *A*, Plot of synchrony distribution with respect to CS activity of master cell (*M*). Synchrony distribution shown for two master cells located in different parasagittal planes, one lateral (*A<sub>1</sub>*) and one more medial (*A<sub>2</sub>*). Circles and the letter *M* represent the relative positions of recorded Purkinje cells on the left crus 2a. The area of each circle is proportional to the degree of synchronous CS activity with cell *M*. Note how the highest levels of synchronization occur in cells located in the same parasagittal plane as cell *M*. *B*, Schematic of dorsocaudal view of cerebellum and medulla showing the position of the recording array. *C*, Cross-correlograms of CS activity in cell *M* in plot of *A<sub>2</sub>* and a cell 500  $\mu$ m rostral to it within the same parasagittal plane (*b*) and a cell located 500  $\mu$ m lateral (*a*). Time bin is 1 msec.

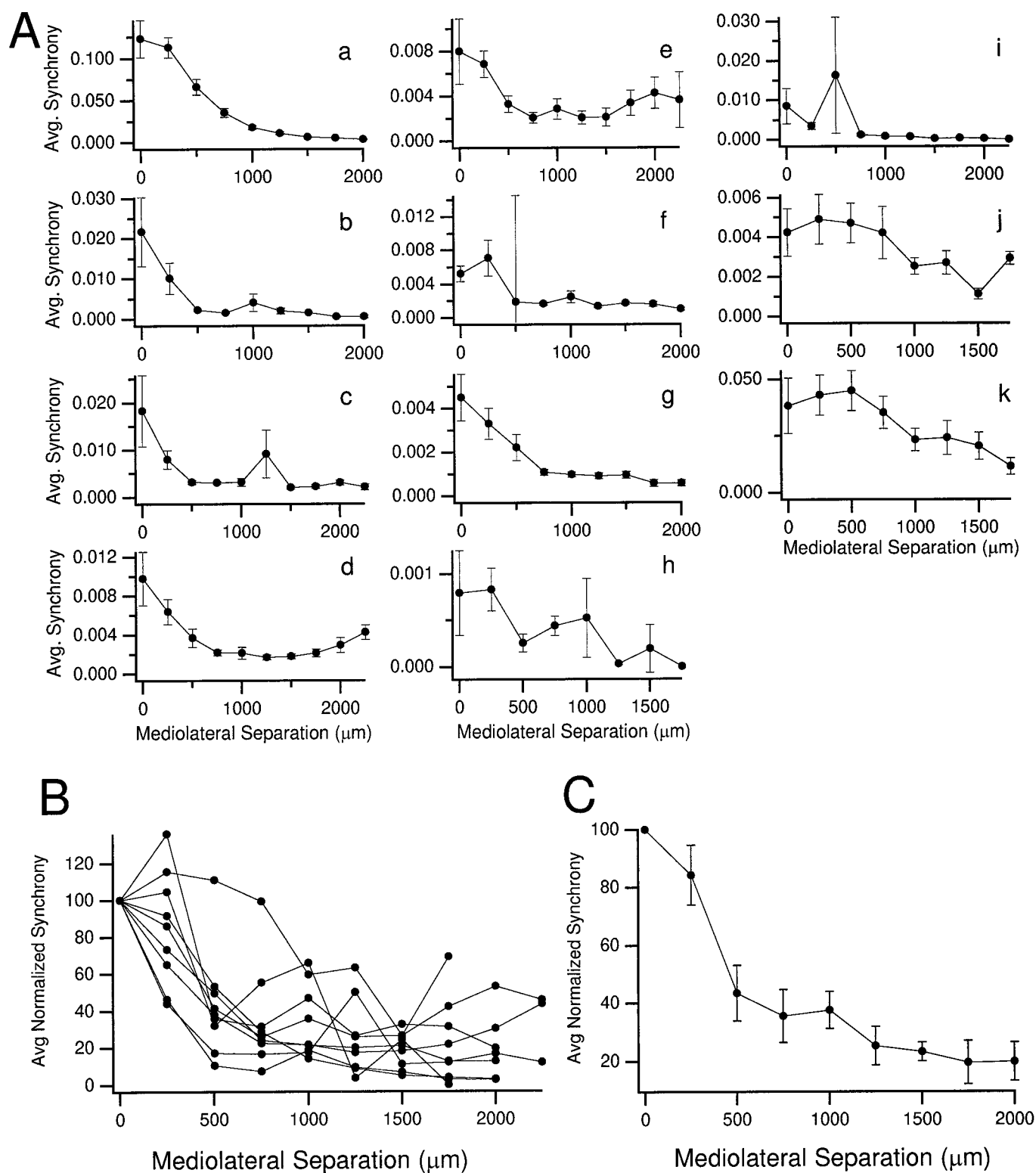


**Figure 2.** Spatial distribution of CS synchrony. *A*, Plots of average level of CS synchrony as a function of mediolateral separation distance between Purkinje cells. Plots from each of the 11 experiments show that CS synchrony decreases with increasing mediolateral separation distance. Plots were obtained by determining  $C(0)$  for all possible cell pairs, sorting cell pairs according to separation distance between cells, and then calculating the mean  $C(0)$  for each separation distance. *B*, Average normalized synchrony as a function of mediolateral separation distance for the nine experiments in which the highest average  $C(0)$  occurred at  $\leq 250 \mu\text{m}$ . All curves are normalized to the  $C(0)$  value at  $0 \mu\text{m}$ . *C*, Average of curves in *B*. Error bars in *A* and *C* indicate SEM.



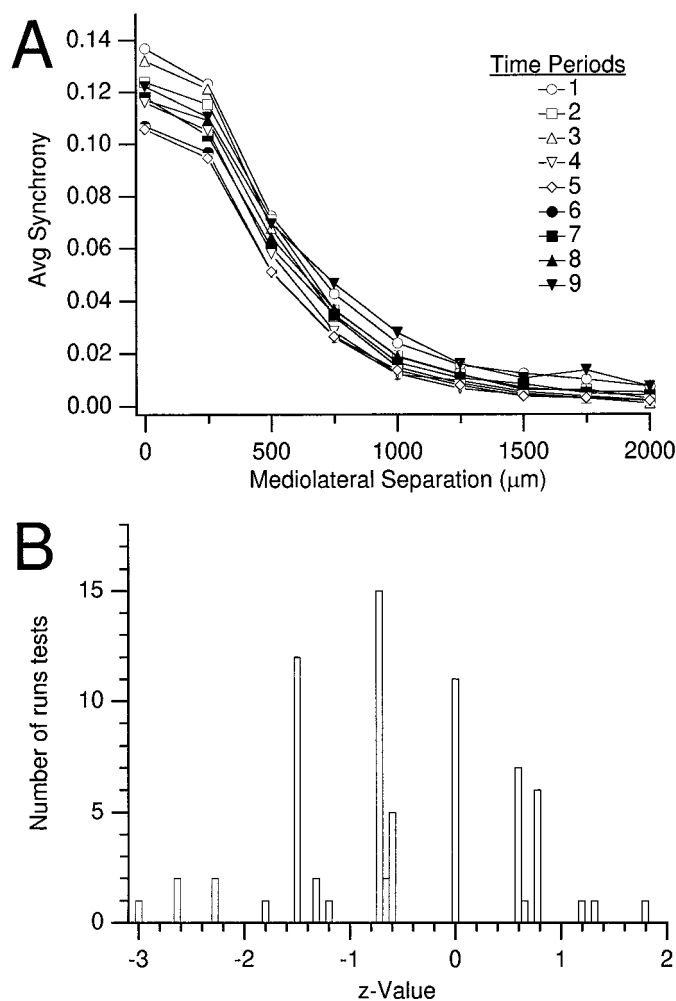


**Figure 3.** Stability of CS synchronicity over time. *A*, Plots of average synchrony as a function of mediolateral separation distance for successive 25 min periods during an  $\approx 4$  hr recording session. Note the constancy of the shape of the curves, despite some fluctuation in absolute levels of synchrony. *B*, Distribution of  $z$  values from runs tests of time sequences of  $C(0)$ .  $z$  values less than  $-1.65$  indicate a statistically significant ( $p < 0.05$ ) trend in the data.

(for example, plot 2*A*c), the particular distribution was present throughout the recording session.

To determine whether the variation in the average level of synchrony was caused by a systematic shift over time, as might occur if the changes were because of residual effects of the anesthesia, or simply random fluctuations, a runs test was performed for the sequence of synchrony values at each mediolateral separation distance. The occurrence of significantly less ( $z < -1.65$ ;  $p < 0.05$ ) runs than expected by chance was taken as evidence of a trend in the data over time. In the experiment shown in Figure 3*A* for all separation distances, the observed number of runs was not significantly less than the expected number due to chance. A total of 71 sequences were analyzed from the eight experiments, and only six (8.45%) were found to contain significantly fewer runs than expected, approximately the percentage of false positives (5%) that should occur given the 0.05 significance level. Moreover, the six sequences that were found to have a statistically significant trend occurred across four experiments, and each occurred at a different mediolateral separation

distance (0, 500, 750, 1000, 1750, and 2000  $\mu\text{m}$ ). The complete distribution of  $z$  values obtained from analysis of the 71 sequences is shown in Figure 3*B*. The distribution was symmetrical with many sequences having greater than or the same number of runs than expected by chance ( $z \geq 0$ ). Thus, the rostrocaudal banding patterns of CS synchrony appear to be relatively stable structures, despite random fluctuations in overall levels of synchrony.

If the parasagittally oriented bands represent functional units of the cerebellar cortex, the level of synchronization within these bands should be relatively stable over time compared with that observed between the CS activity of Purkinje cells located in different parasagittal planes. This was verified by calculating the coefficient of variation ( $CV = SD/\text{mean}$ ) as a measure of the relative variation in the average synchrony. For each experiment ( $n = 8$ ), the CV was determined for each temporal sequence of synchrony values and plotted as a function of the mediolateral separation distance of the sequence (Fig. 4). In all experiments, the CV increased with increasing separation distance, resulting in a positive correlation ( $r = 0.80 \pm .09$ ; range, 0.66 to 0.96). In six of eight experiments the correlation was statistically significant ( $p < 0.05$ ).

### CS rhythmicity in the awake animal

The extent to which spontaneous CS activity is rhythmic in awake animals was studied by constructing autocorrelograms ( $n = 282$ ). Visual inspection of these correlograms showed that rhythmic activity was present in the large majority of cells. Typically, the autocorrelograms displayed a prominent primary peak followed by one or more smaller higher order peaks at regularly spaced intervals, such as those shown in Figure 5, *B* and *C*. The RIs for the autocorrelograms of Figure 5, *B* and *C*, were 0.0207 and 0.0260, respectively. In some cells, the CS activity displayed a more pronounced rhythmicity, such as the example shown in Figure 5*D* (RI = 0.0986). In contrast, only  $\approx 4\%$  of the cells lacked any evidence of rhythmic activity as defined by the absence of any significant peaks (see Fig. 8*A*), and an additional 18% had relatively weak rhythmicity ( $0 < \text{RI} < 0.01$ ). Thus, in total only  $\approx 22\%$  of the cells could be characterized as having weak or absent rhythmicity (see Fig. 8*B*). The autocorrelogram of one such cell, which had an RI of 0.0088, is shown in Figure 5*A*. Analysis of the entire population ( $n = 282$  cells) showed that the autocorrelograms had  $2.91 \pm 1.84$  peaks and an RI of  $0.0332 \pm 0.0377$  on average, both of which were significantly ( $p < 0.001$ ) greater than zero. The distributions of the peak number and RI are shown in Figure 8 (*histogram bars*). Note that although  $\approx 77\%$  of the autocorrelograms displayed two or more peaks, indicating a sustained oscillation for at least several cycles, 19% showed only a single significant peak. However, even these latter autocorrelograms indicate the presence, however transient, of an  $\approx 10$  Hz rhythmicity and not simply a modal interval caused by the average firing rates of the cells.

The variation in the strength of rhythmic activity over time was calculated for each of the eight experiments in which continuous recordings were obtained for  $\approx 4$  hr by dividing each experiment into successive 25 min periods. Analysis of the autocorrelograms from the successive periods showed that there was some variation in the average number of peaks and in the RI. An example of this variation is shown in Figure 6, where the values of these parameters in one experiment are plotted for successive 25 min periods. Similar variability was observed in each of the experiments; however, this variation was random in nature, because runs tests

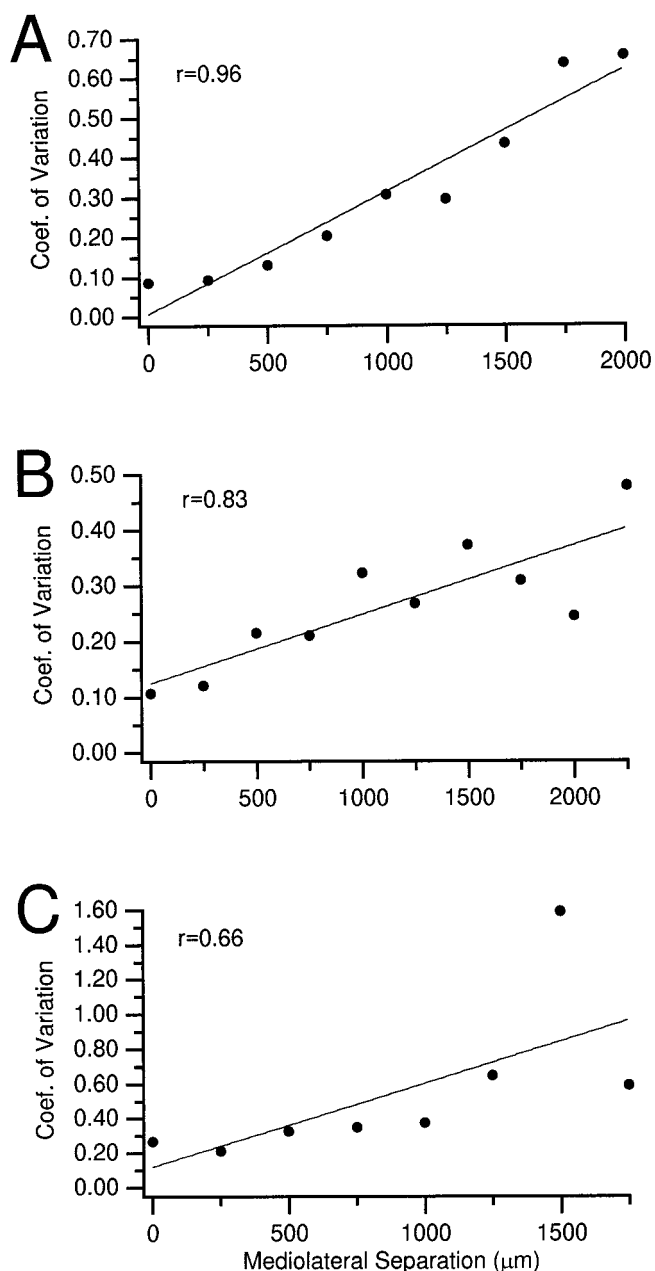


**Figure 4.** Relative stability of intraband synchrony. Plots of CV as a function of mediolateral separation distance. CV was positively correlated with mediolateral separation distance. *A–C* show results from the three experiments in which the strongest, the average, and the weakest relationship was found, respectively. The correlation ( $r$ ) was significant ( $p < 0.05$ ) for *A* and *B*.

for peak number and RI gave  $p$  values that were not significant in all but 1 of 16 cases (6.25%). Runs tests for the mean number of peaks yielded  $z$  values of  $-0.7548 \pm 0.7169$  ( $n = 8$ ) on average, whereas for the RI the  $z$  values averaged only  $-0.0418 \pm 0.8691$  ( $n = 8$ ).

Most of the present recordings were obtained from long ( $\approx 4$  hr) sessions in which each cell had on the order of 10,000–20,000 CSs. The relatively long recordings probably facilitated our observing the CS rhythmicity and may, in part, explain the differences in the present results from those of Keating and Thach (1995). In particular, the variations in rhythmicity during the long

recording sessions suggested the possibility that CS rhythmicity could be missed with shorter duration recordings. Thus, we asked the following question: for a cell that shows significant rhythmicity during the entire recording session (i.e.,  $R \geq 0.01$ ), what is the probability of failing to detect any rhythmicity (i.e., no significant peaks or  $RI = 0$ ) in a shorter duration recording? To answer this question, a long recording session ( $\approx 250$  min) was divided into shorter duration segments (25, 10, 5, and 2.5 min segments). The RI was then calculated for each cell for every segment. Next, for each cell that displayed significant rhythmicity ( $RI \geq 0.01$ ) during the entire recording session, the probability that it displayed no rhythmicity ( $RI = 0$  or equivalently no significant peaks in the autocorrelogram) was calculated for each segment duration. For example, the recording session was divided into ten 25 min segments. If a cell had an  $RI = 0$  for one of those segments, the probability of failing to detect its rhythmicity in 25 min duration recordings was 10%. The results of this analysis for an experiment in which 24 cells displayed rhythmicity ( $RI \geq 0.01$ ) for the entire recording session are shown in Figure 7. Each histogram plots the probability of failing to detect rhythmicity (i.e., number of segments with  $RI = 0$ ) for recording segments of a given duration. For the shorter duration segments (2.5 and 5 min), only  $\approx 8$  and 30% of the cells had little to no chance (0–5%) of failing to detect the rhythmicity, as indicated by the leftmost bins of the corresponding histograms in Figure 7. Nevertheless, the distributions of these histograms indicate that there is a relatively low chance of missing the rhythmicity. For the 2.5 min segments there was a  $21.7 \pm 14.9\%$  chance of missing the rhythmicity on average, and for the 5 min segments a  $17.9 \pm 14.7\%$  chance. When the duration of the recording segment was increased, these percentages fell further to  $12.7 \pm 13.4\%$  for the 10 min segments and  $7.5 \pm 9.9\%$  for the 25 min segments. Note that for the 25 min segments there was virtually no chance of failing to detect the rhythmicity in over half of the population (leftmost bin in this histogram corresponds to 0% only, because there were only ten such segments and one failure would give a value of 10%). The few ( $n = 5$ ) cells with more than one segment in which rhythmicity was not detected for the 25 min segments had very low firing rates (range, 0.1–0.34 Hz), which correspond to relatively short spike trains of 150–510 spikes for 25 min recordings.

The results indicate that recordings of 10–25 min are needed to be confident that CS rhythmicity, when present, will be detected. The average firing rate for this experiment was 0.60 Hz, which corresponds to an average spike train of 360–900 spikes for recordings of 10 and 25 min, respectively. This suggests that CS rhythmicity may be missed if autocorrelograms are generated from spike trains containing fewer spikes. It should also be mentioned that in two of our awake animals, as well as in the seven anesthetized animals, the entire recording sessions were of short duration (15–30 min), yet the rhythmicity of the CS activity was evident in the autocorrelograms and RIs of cells in these experiments. Consistent with these values, we generally find that to observe the rhythmicity in the autocorrelograms clearly by eye, spike trains must contain at least 300–500 spikes, although in cells displaying a strong rhythmicity less spikes are needed.

Given that most Purkinje cells displayed rhythmic CS activity, it became of interest to investigate the preferred oscillation frequencies displayed by spontaneous CS activity in the waking animal. The oscillation frequency for each cell was calculated as the reciprocal of the interval from  $t = 0$  to the first peak in its autocorrelogram. The oscillation frequency was only determined for cells displaying significant rhythmicity (RIs of  $\geq 0.01$ ). Thus,

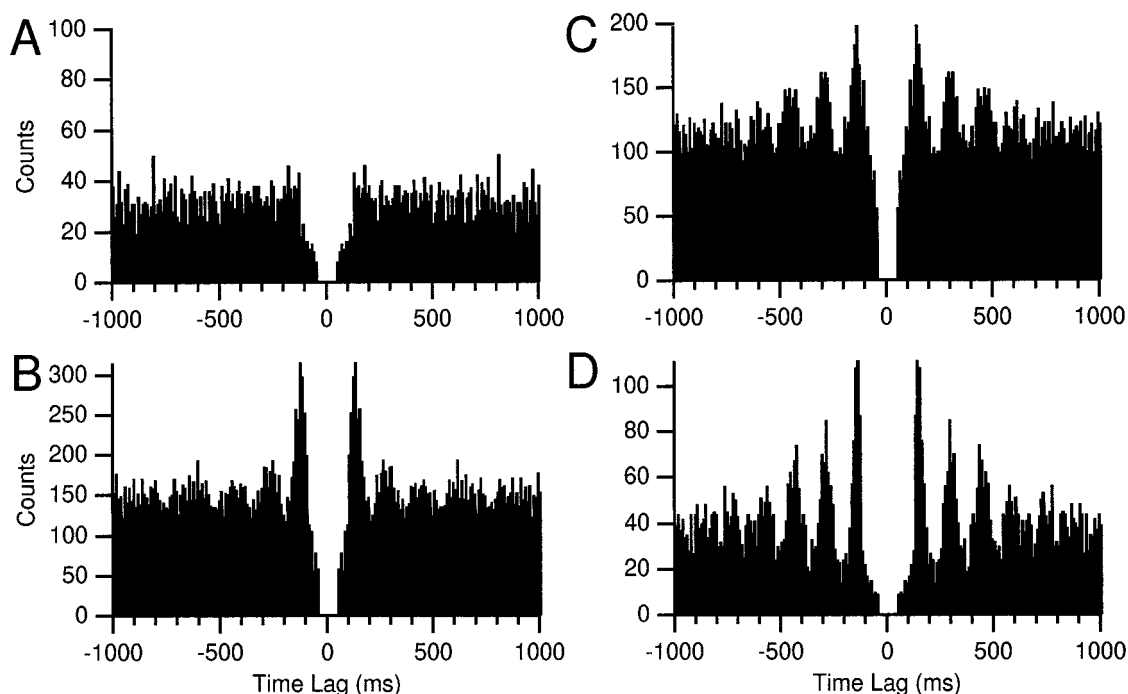


**Figure 5.** Autocorrelograms of CS activity. Autocorrelograms of CS activity from four Purkinje cells showing the range of rhythmicity present. *A*, Example of CS activity displaying little rhythmicity ( $RI = 0.0088$ ). *B*, *C*, Cells showing more typical rhythmic activity ( $RI$ s = 0.0207, 0.0260). *D*, Example of strongly rhythmic CS activity ( $RI = 0.0986$ ). Bin width of histogram is 10 msec.

cells with autocorrelograms such as shown in Figure 5*A* were excluded, whereas cells with correlograms similar to those in Figure 5*B–D* were included. Frequency analysis was performed on eight experiments in which the majority of cells in each case showed  $RI$ s  $\geq 0.01$ . Overall, 177 of 215 cells (82.3%) in these experiments met the criteria for oscillation frequency determination. The average oscillation frequency for these cells was  $10.27 \pm 2.89$  Hz. A large amount of the variation was caused by differences between experiments. That is, the average oscillation frequency in the different animals ranged from 7.03–13.31 Hz, and the average of the individual animal SDs was 1.68 compared with the overall SD of 2.89.

#### Comparison of CS activity in anesthetized and awake animals

The similarity or difference of the functional state of the olivocerebellar system under ketamine–xylazine anesthesia as compared with the unanesthetized condition was determined by characterizing the rhythmicity and synchronicity of CS activity in the two states. The  $\approx 10$  Hz oscillation frequency observed in the waking state is very similar to what has been reported previously under anesthesia (Sasaki et al., 1989; Lang et al., 1997). Moreover, as shown by the peak number and  $RI$  distributions (Fig. 8), the strength of the rhythmicity was similar in the two states. Although the  $RI$  distribution from the activity in awake animals appears somewhat shifted to the left relative to that from anesthetized animals, the means of the  $RI$  distributions for anesthetized ( $0.0358 \pm 0.0268$ ;  $n = 257$ ) and unanesthetized ( $0.0332 \pm 0.0377$ ;  $n = 282$ ) animals were similar. In addition, the mean of the peak distribution was higher for cells recorded in unanesthetized animals ( $2.91 \pm 1.84$ ;  $n = 282$ ) than for those recorded in anesthetized animals ( $1.99 \pm 1.17$ ;  $n = 257$ ).

With regard to CS synchronicity, the parasagittal banding pattern observed in the waking state was similar to what has been

observed under ketamine–xylazine anesthesia. A direct comparison of the anesthetized and nonanesthetized synchrony distributions was performed by determining the normalized synchrony distribution from seven experiments performed under anesthesia (Fig. 9*A*) and comparing the average normalized synchrony curve from these experiments to that found for the nonanesthetized animals (Fig. 9*B*). The similarity of the curves in Figure 9*B* indicates that the predominant patterns of CS synchrony that have been previously described under ketamine–xylazine anesthesia are the same as those observed in the waking animal.

#### DISCUSSION

The ability of the olivocerebellar system to generate rhythmic synchronous discharges has been proposed to play a central role in motor coordination (Llinás, 1974, 1991). Yet although the rhythmic and synchronous nature of spontaneous olivocerebellar activity has been documented in anesthetized animals and in *in vitro* preparations, there has been no quantitative description of these characteristics of spontaneous olivocerebellar activity in the waking state. Thus, we performed multiple electrode recordings of spontaneous CS activity from lobule crus 2a in awake animals. Our results demonstrate that in the awake animal the olivocerebellar system generates synchronous CS activity and that the predominant spatial distribution is similar to what has been described in anesthetized animals (i.e., synchronous CS activity occurs mainly among Purkinje cells located within parasagittally oriented strips of cortex). Furthermore, we found that the large majority of Purkinje cells within crus 2a display rhythmic CS activity with an  $\approx 10$  Hz periodicity.

#### Parasagittal organization of CS synchrony

The neurons of the inferior olive are characterized not only by their intrinsic oscillatory electrical activity, which results from the interplay between different voltage-dependent calcium and potas-



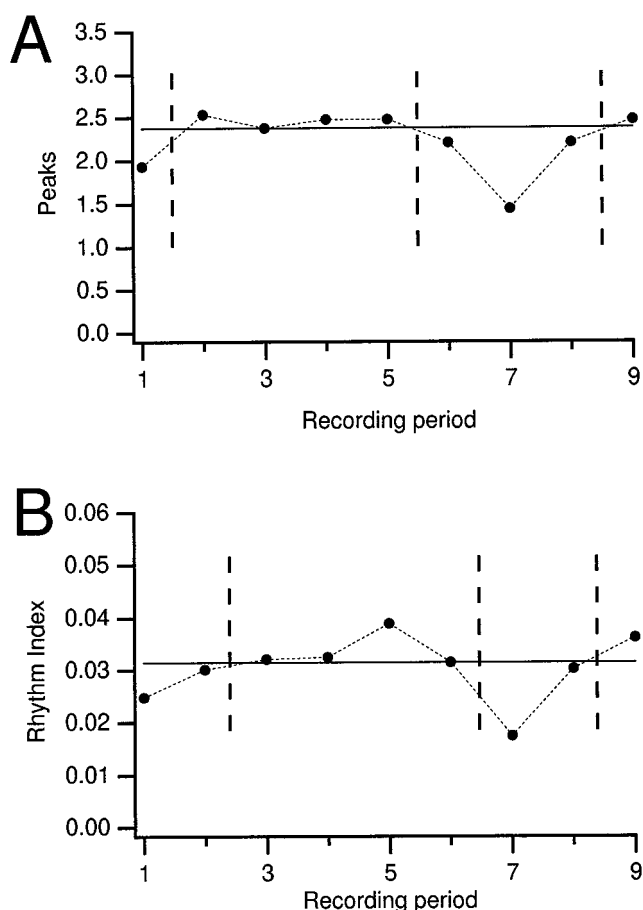


**Figure 6.** Variation of rhythmicity over time. Plot of average number of peaks (*A*) and average value of RI (*B*) for successive 25 min periods from one experiment in which 29 cells were simultaneously recorded. Horizontal lines indicate median values. Points of crossing of median indicated by vertical dashed lines.

sium conductances (Llinás and Yarom, 1981a,b), but in addition, are electrotonically coupled via gap junctions located within glomeruli (Llinás et al., 1974; Sotelo et al., 1974). Indeed, the inferior olive has the highest known density of neuronal gap junctions within the mammalian CNS (de Zeeuw et al., 1995) and thus contains the anatomical substrate for generating simultaneous electrical discharges, which in turn could result in synchronous CS activity throughout the cerebellar cortex. The potential for such global synchronization is shown by the fact that synchronous CS activity has been observed between Purkinje cells located in widely separated regions of the cerebellar cortex (Wylie et al., 1995; de Zeeuw et al., 1996). However, despite this potential, in anesthetized animals synchronous CS activity is typically observed primarily among Purkinje cells located within parasagittally oriented strips of cortex (Bell and Kawasaki, 1972; Llinás and Sasaki, 1989; Sasaki et al., 1989). Although these strips may be quite long, extending not just across the apex of a folium, but also down its walls (Sugihara et al., 1993) and across successive folia (E. Lang, I. Sugihara, and R. Llinás, unpublished observations), they nevertheless are typically narrow structures with a width of only 250–500  $\mu\text{m}$ . The localization of the gap junctions within glomeruli has suggested that the functional coupling of IO neurons is modulated at those sites by inhibitory input and could therefore underlie the limited spatial distribution of CS synchrony that is normally observed (Llinás, 1974). Recent experiments have provided support for this idea by demonstrating that blocking the activity of the GABAergic cerebellar nucleo-olivary pathway produces widespread synchronization of CS activity (Lang et al., 1996).

The results of the present investigation indicate that the spatial distribution of spontaneous CS synchrony is similarly restricted in the awake animal. In all animals, CS synchrony was greater on average for Purkinje cells with smaller mediolateral separation distances than for those separated by large distances. In fact, in most animals high levels of synchrony were limited to Purkinje cells separated by 250  $\mu\text{m}$  or less, with a rapid reduction of synchronous activity occurring between 250 and 500  $\mu\text{m}$ . Thus, in awake animals in crus 2a, synchronous CS activity occurs primarily among Purkinje cells located within narrow parasagittally oriented strips of cortex, suggesting the existence of functional

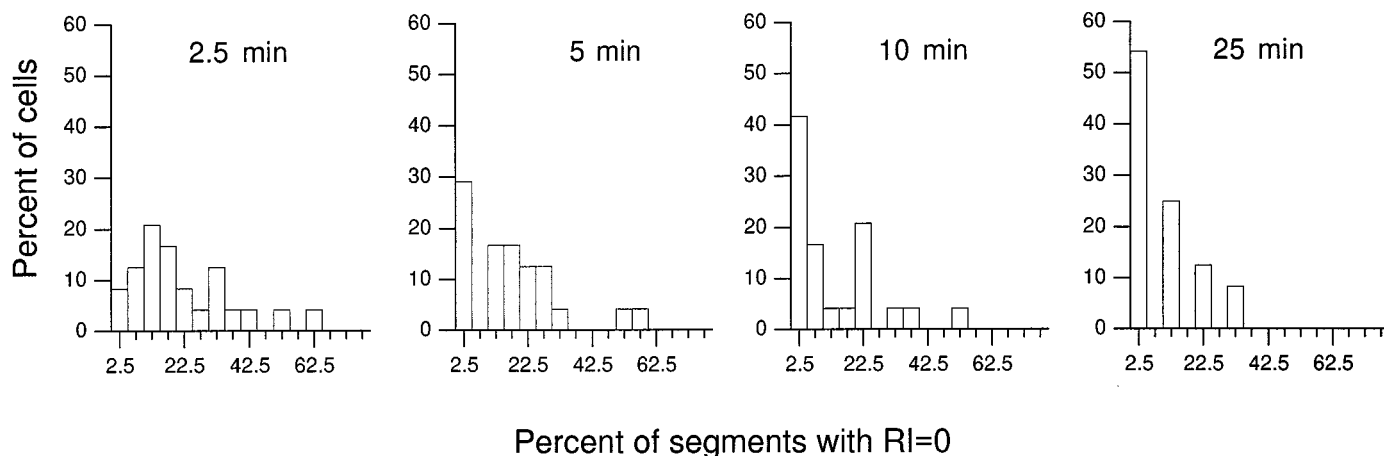


**Figure 7.** Probability of failing to detect CS rhythmicity in short duration recordings. Each histogram plots the percent of cells as a function of the percent of recording segments in which CS rhythmicity was not detected for segments of a particular duration. Duration of recording segments indicated above each histogram. Histogram bin width is 5%. Centers of bins are indicated by x-axis label. The analysis was performed on  $n = 24$  cells. The segments were obtained by dividing an  $\approx 4$  hr recording session into nonoverlapping pieces. The number of segments used was 88, 49, 24, and 10 for the 2.5, 5, 10, and 25 min durations, respectively.

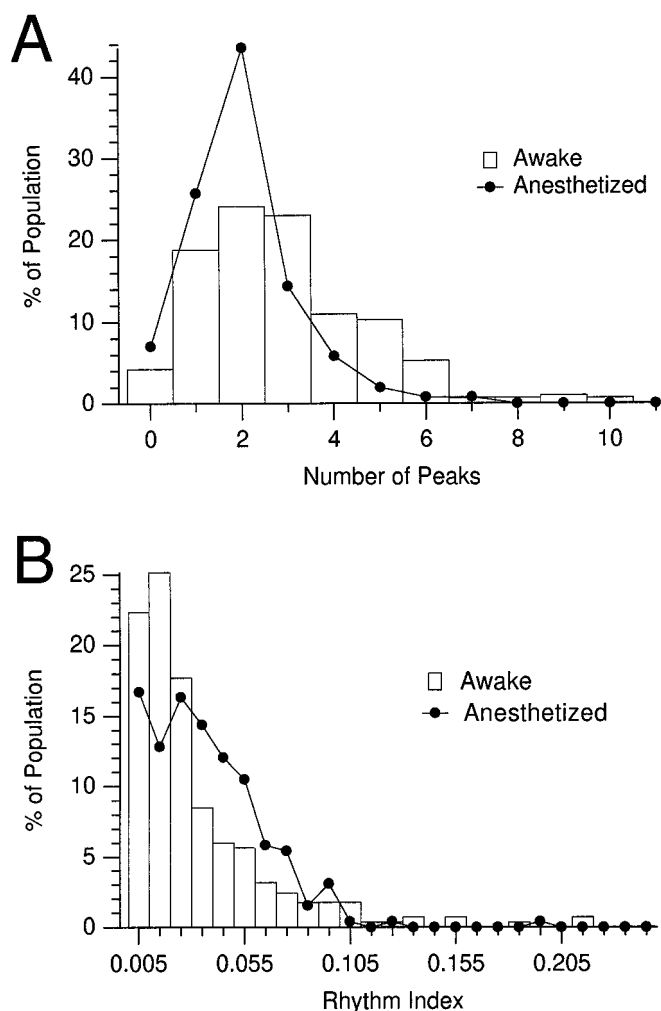


**Figure 8.** Comparison of CS rhythmicity in awake and anesthetized states. *A*, Distribution of number of significant peaks shown by autocorrelograms of CS activity in awake (histogram bars;  $n = 282$  cells) and anesthetized (filled circles;  $n = 257$  cells) animals. *B*, Distribution of RI in awake (histogram bars) and anesthetized (filled circles) animals.

corticonuclear domains in accordance with the rostrocaudal organization of Purkinje cell innervation of the cerebellar nuclei (Cicirata et al., 1992).

It is theoretically possible that the similarity of the awake patterns to the anesthetized ones, rather than reflecting the normal organization of CS synchrony, could have been caused by the residual effect of the ketamine anesthesia used during electrode implantation. We consider this possibility unlikely for the following reasons. First, ketamine is a relatively short ( $\approx 30$  min)-lasting anesthetic (Flecknell, 1996), and the recordings always began several hours after anesthetization and lasted for  $\approx 4$  hr after that in most cases. Second, during recovery from the anesthesia the animals typically pass through a light anesthetic state during which highly synchronous and rhythmic CS activity and tremor-like movements occur (Lang, 1995). During this period, the spatial organization of CS synchrony and rhythmicity is different from that observed under the usual anesthetic conditions and also different from that in the fully awake animal capable of performing behavioral tasks. Third, analyses of the spatial distribution of synchrony and rhythmicity from successive time periods during the  $\approx 4$  hr recording sessions failed to disclose any system-

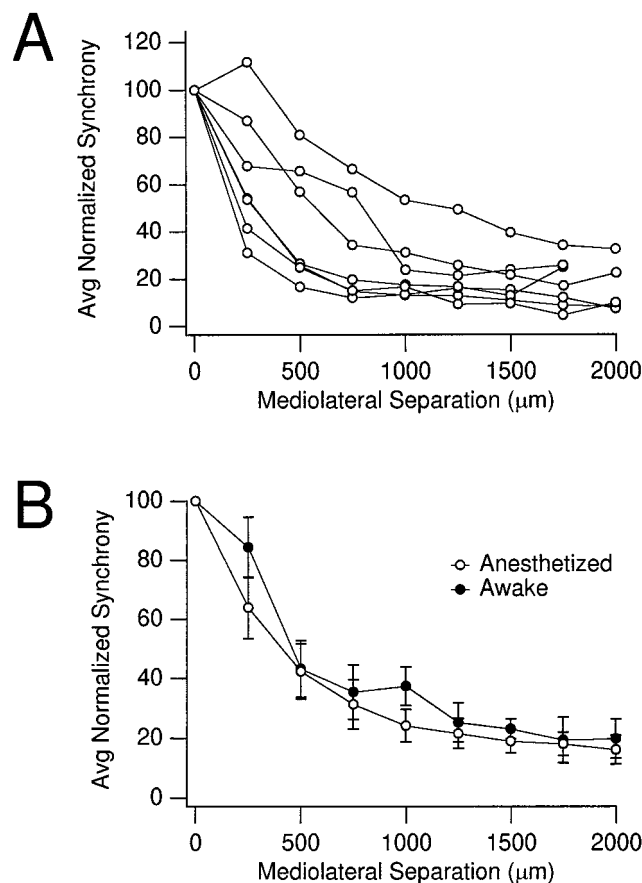


**Figure 9.** Comparison of CS synchronicity in awake and anesthetized states. *A*, Average normalized synchrony plotted as a function of mediolateral separation distance for seven experiments in ketamine-xylazine-anesthetized rats. *B*, Plot of average curve (open circles) from the seven experiments shown in *A*. For comparison, the average curve of Figure 2C obtained from the awake animals is replotted (filled circles). Error bars indicate SEM.

atic trends that would be indicative of the wearing off of the anesthetic. Finally, in most animals the data were obtained during a recording session in which the animal was capable of accurately performing complex movements, which would not have been possible if there were a continuing significant action of the anesthetic on cerebellar activity. Moreover, significant changes in the patterns of synchronous CS activity were observed in relation to the movements that were performed during the recording session (Welsh et al., 1995a). Thus, the olivocerebellar system was capable of generating alternative functional patterns.

Questions then arise concerning the functional significance of these parasagittal bands, particularly in relation to movement-related patterns of activity. That these bands are functional entities is supported by the constancy of the banding structure over time and by the fact that the mean synchrony levels among Purkinje cells located within the same parasagittal strip demonstrated less time variation than did those of Purkinje cells separated in the mediolateral axis. That is, the CS activity of Purkinje cells within a band appeared to be strongly coherent, as would be expected if they formed a functional unit. It seems plausible then, particularly given the somatotopic organization of the motor output of the cerebellar nuclei (Cicirata et al., 1992), to postulate that the activity of each band of cells would function to control a small group of related muscles or a well defined motor synergy

(Lang, 1995). The CS synchrony patterns observed during movements would then result from the coupling of activity from the various parasagittal bands that control the muscle groups needed to perform particular movements.

### Spontaneous 10 Hz rhythmicity in olivocerebellar activity

It is clear that under anesthetized conditions or in *in vitro* preparations, the olivocerebellar system can generate rhythmic activity spontaneously (de Montigny and Lamarre, 1973; Llinás and Volkind, 1973; Belcarì et al., 1977; Llinás and Yarom, 1981a,b, 1986; Benardo and Foster, 1986; Llinás and Sasaki, 1989; Sasaki et al., 1989; Lampl and Yarom, 1993, 1997; Sugihara et al., 1995; Wylie et al., 1995; Lang et al., 1996, 1997). Moreover, this rhythmic activity has been recorded from both vermal and hemispheric regions (Sugihara et al., 1995) and from several of the olivary subnuclei (Llinás and Yarom, 1981a,b), suggesting that it is typical of olivocerebellar activity generally and not characteristic of the activity of a particular division of this system.

However, there has been some debate concerning the presence of rhythmic CS activity in the alert animal (Keating and Thach, 1995). The present results should help to resolve this debate because they provide clear evidence that the large majority of crus 2a Purkinje cells display spontaneous  $\approx 10$  Hz rhythmic CS activity in the awake animal. The present findings are consistent with early investigations of CS activity in awake animals, which briefly reported the presence of rhythmic CS activity (Rushmer and Woodward, 1971; Bell and Kawasaki, 1972), as well as with our previous work demonstrating rhythmic movement-related CS activity (Welsh et al., 1995a).

Our data are also in general agreement with those of Pellerin et al. (1997), who described the occurrence of rhythmic CS activity in behaving primates. These authors, however, reported that only  $\sim 45\%$  of Purkinje cells displayed evidence of rhythmic CS activity, whereas in our population  $>90\%$  showed at least some evidence of such activity. Part of this difference may be ascribable to analytic methodology (we detected peaks in autocorrelograms, whereas they analyzed the Fourier transforms of the averaged autocorrelograms from repeated trials in their task). More likely this difference reflects the fact that the olivocerebellar system must be in a distinct functional state when the animal performs a movement as compared with when it is remaining still, such that there is a differential modulation of the rhythmicity of distinct subgroups of IO neurons during the movement. That is, generation of a movement results from pulsatile activation of a specific set of muscles (Vallbo and Wessberg, 1993). If, as we hypothesize, the periodic synchronous discharges of the olivocerebellar system help organize these pulsatile motor commands, during a movement there should be an upregulation of the rhythmicity of IO neurons that help control the muscles that need to be contracted and a downregulation of the rhythmicity of other IO neurons that control muscles that must relax.

Our results, and those of Pellerin et al. (1997), differ significantly from those of Keating and Thach (1995), who were unable to detect rhythmicity in the CS activity recorded from primates performing motor tasks. These differences are not likely to be caused by species differences, because the recordings of Pellerin et al. (1997) were also from primates. An explanation probably resides, in part, in the analytical methodology used by Keating and Thach (1995). In particular, their concatenation method for generating CS autocorrelograms introduced false random interspike intervals into their data sets, which would obscure a 10 Hz

signal (as they themselves admit in a subsequent paper, see Methods section of Keating and Thach, 1997). The effect of this error can be observed in their Figure 3 (Keating and Thach, 1995) in which rhythmic movement-related CS activity is readily observed in the raster display of the raw data but barely visible in the corresponding autocorrelogram. An additional factor in their failure to detect CS rhythmicity may have been the relatively small data sets used by Keating and Thach (1995). Their recordings ranged between 102 and 3643 intervals. Most of our recordings contained spike trains consisting of 5000–25,000 spikes. Analysis of short segments of these spike trains (Fig. 7) indicated that the rhythmicity might not be detected if the number of spikes in a train dropped below 400–900. Thus, for at least some percentage of their cells, the ability of Keating and Thach (1995) to detect CS rhythmicity may also have been compromised by their limited data sets.

Given that the olivocerebellar system generates a periodic activation of the cerebellar cortex, the issue arises as to whether there is also periodic modulation of cerebellar output at the nuclear level, as would be required for the proposed timing role of the olivocerebellar system in motor coordination. It is clear that when pharmacologically enhanced, the activity of the olivocerebellar system does produce a rhythmic activation of the cerebellar nuclei, one which leads to phase-locked motor activity (de Montigny and Lamarre, 1973; Llinás and Volkind, 1973). However, under more physiological conditions, Keating and Thach (1997) have failed to observe any periodicity indicative of olivocerebellar discharge in the movement-related activity of cerebellar nuclear neurons. This failure may have been caused by the limitations of the single-unit recording technique used, because during normal movements the rhythmic activation of a single cell is likely to be subtle, because pronounced rhythmic activation of cerebellar nuclear neurons results in a large amplitude tremor. This subtle modulation may not be detectable in the single-unit recordings because activity generated by the olivocerebellar system is likely to be buried within activity caused by other cerebellar nuclear afferents. Nevertheless, there could still be a significant alteration of activity across the population as a whole because of the synchronous nature of olivocerebellar discharges. Indeed, as we have argued, the olivocerebellar system is not designed to produce its effects by generating large changes in single cell firing rates, which would be readily detectable with single-unit recordings, but rather by changes in the pattern of activity across populations of cells. Thus, testing whether the olivocerebellar system, which produces rhythmic and synchronous activation of the cerebellar cortex, also produces a periodic activation of the cerebellar nuclei may require the use of techniques, such as multiple electrode recordings, that measure the population response of the cerebellar nuclei.

### Functional significance of the olivocerebellar synchrony and rhythmicity

The demonstration of synchronous and rhythmic CS activity in the awake animal provides further support that these characteristics of olivocerebellar activity have functional significance. The present results are also consistent with the hypothesis that the olivocerebellar system may subserve a timing function for organizing the activation of muscle synergies needed to generate movements. Although at present we can only speculate on the specific functional relationship of the parasagittal bands of synchronous CS activity to motor output, their presence and the

unquestionable anatomical and functional organization of the olivary complex provides strong evidence that the olivocerebellar system has evolved to contribute significantly and directly to the output of the cerebellar cortex and nuclei.

## REFERENCES

- Armstrong DM, Rawson JA (1979) Activity patterns of cerebellar cortical neurones and climbing fiber afferents in the awake cat. *J Physiol (Lond)* 289:425–448.
- Belcari P, Francesconi A, Maioli C, Strata P (1977) Spontaneous activity of Purkinje cells in the pigeon cerebellum. *Pflügers Arch* 371:147–154.
- Bell CC, Kawasaki T (1972) Relations among climbing fiber responses of nearby Purkinje cells. *J Neurophysiol* 35:155–169.
- Benardo LS, Foster RE (1986) Oscillatory behavior in inferior olive neurons: mechanisms, modulation, cell aggregates. *Brain Res Bull* 17:773–784.
- Bloedel JR, Ebner TJ (1984) Rhythmic discharge of climbing fibre afferents in response to natural peripheral stimuli in the cat. *J Physiol (Lond)* 352:129–146.
- Cicirata F, Angaut P, Serapide MF, Panto MR, Nicotra G (1992) Multiple representation in the nucleus lateralis of the cerebellum: an electrophysiologic study in the rat. *Exp Brain Res* 89:352–362.
- de Montigny C, Lamarre Y (1973) Rhythmic activity induced by harmaline in the olivo-cerebello-bulbar system of the cat. *Brain Res* 53:81–95.
- de Zeeuw CI, Holstege JC, Ruigrok TJH, Voogd J (1989) Ultrastructural study of the GABAergic, cerebellar, and mesodiencephalic innervation of the cat medial accessory olive: anterograde tracing combined with immunocytochemistry. *J Comp Neurol* 284:12–35.
- de Zeeuw CI, Hertzberg EL, Mugnaini E (1995) The dendritic lamellar body: a new neuronal organelle putatively associated with dendrodendritic gap junctions. *J Neurosci* 15:1587–1604.
- de Zeeuw CI, Lang EJ, Sugihara I, Ruigrok TJH, Voogd J (1996) Morphological correlates of bilateral synchrony in the rat cerebellar cortex. *J Neurosci* 16:3412–3426.
- Flecknell P (1996) *Laboratory Animal Anesthesia*, 2nd ed. London: Academic Press.
- Hobson JA, McCarley RW (1972) Spontaneous discharge rates of cat cerebellar Purkinje cells in sleep and waking. *Electroencephalogr Clin Neurophysiol* 33:457–469.
- Keating JG, Thach WT (1995) Nonclock behavior of inferior olive neurons: interspike interval of Purkinje cell complex spike discharge in the awake behaving monkey is random. *J Neurophysiol* 73:1329–1340.
- Keating JG, Thach WT (1997) No clock signal in the discharge of neurons in the deep cerebellar nuclei. *J Neurophysiol* 77:2232–2234.
- Lampl I, Yarom Y (1993) Subthreshold oscillations of the membrane potential: a functional synchronizing and timing device. *J Neurophysiol* 70:2181–2186.
- Lampl I, Yarom Y (1997) Subthreshold oscillations and resonant behavior: two manifestations of the same mechanism. *Neuroscience* 78:325–341.
- Lang EJ (1995) Synchronicity, Rhythmicity and movement: the role of the olivocerebellar system in movement. PhD thesis, NYU Medical Center.
- Lang EJ, Sugihara I, Llinás R (1996) GABAergic modulation of complex spike activity by the cerebellar nucleoolivary pathway in rat. *J Neurophysiol* 76:255–275.
- Lang EJ, Sugihara I, Llinás R (1997) Differential roles of apamin and charybdotoxin sensitive  $K^+$  conductances in the generation of inferior olive rhythmicity *in vivo*. *J Neurosci* 17:2825–2838.
- Llinás R (1974) Eighteenth Bowditch lecture. Motor aspects of cerebellar control. *Physiologist* 17:19–46.
- Llinás R (1991) The noncontinuous nature of movement execution. In: *Motor control: concepts and issues* (Humphrey DR, Freund H, eds), pp 223–242. New York: Wiley.
- Llinás R, Sasaki K (1989) The functional organization of the olivocerebellar system as examined by multiple Purkinje cell recordings. *Eur J Neurosci* 1:587–602.
- Llinás R, Volkind RA (1973) The olivo-cerebellar system: functional properties as revealed by harmaline-induced tremor. *Exp Brain Res* 18:69–87.
- Llinás R, Yarom Y (1981a) Electrophysiology of mammalian inferior olivary neurones *in vitro*. Different types of voltage-dependent ionic conductances. *J Physiol (Lond)* 315:549–567.
- Llinás R, Yarom Y (1981b) Properties and distribution of ionic conductances generating electroresponsiveness of mammalian inferior olivary neurones *in vitro*. *J Physiol (Lond)* 315:569–584.
- Llinás R, Yarom Y (1986) Oscillatory properties of guinea-pig inferior olivary neurones and their pharmacological modulation: an *in vitro* study. *J Physiol (Lond)* 376:163–182.
- Llinás R, Baker R, Sotelo C (1974) Electrotonic coupling between neurons in cat inferior olive. *J Neurophysiol* 37:560–571.
- Mano N-I (1970) Changes of simple and complex spike activity of cerebellar Purkinje cells with sleep and waking. *Science* 170:1325–1327.
- Pellerin J-P, Parent M-T, Valiquette C, Lamarre Y (1997) Rhythmic climbing fiber responses in the cerebellum of the awake behaving monkey. *Soc Neurosci Abstr* 23:1286.
- Rushmer DS, Woodward DJ (1971) Responses of Purkinje cells in the frog cerebellum to electrical and natural stimulation. *Brain Res* 33:315–335.
- Sasaki K, Bower JM, Llinás R (1989) Multiple Purkinje cell recording in rodent cerebellar cortex. *Eur J Neurosci* 1:572–586.
- Simpson JI, Wylie DR, De Zeeuw CI (1996) On climbing fiber signals and their consequence(s). *Behav Brain Sci* 19:384–398.
- Soechting JF, Ranish NA, Palminteri R, Terzuolo CA (1976) Changes in a motor pattern following cerebellar and olivary lesions in the squirrel monkey. *Brain Res* 105:21–44.
- Sotelo C, Llinás R, Baker R (1974) Structural study of inferior olivary nucleus of the cat: morphological correlates of electrotonic coupling. *J Neurophysiol* 37:541–559.
- Sugihara I, Lang EJ, Llinás R (1993) Uniform olivocerebellar conduction time underlies Purkinje cell complex spike synchronicity in the rat cerebellum. *J Physiol (Lond)* 470:243–271.
- Sugihara I, Lang EJ, Llinás R (1995) Serotonin modulation of inferior olivary oscillations and synchronicity: a multiple-electrode study in the rat cerebellum. *Eur J Neurosci* 7:521–534.
- Vallbo AB, Wessberg J (1993) Organization of motor output in slow finger movements in man. *J Physiol (Lond)* 469:673–691.
- Welsh JP, Lang EJ, Sugihara I, Llinás R (1995a) Dynamic organization of motor control within the olivocerebellar system. *Nature* 374:453–457.
- Welsh JP, Lang EJ, Marquez R, Sugihara I (1995b) Dynamic modulation of olivocerebellar rhythmicity during arm-tongue movement sequences. *Soc Neurosci Abstr* 21:271.
- Wonnacott TH, Wonnacott RJ (1977) *Introductory statistics*, Ed 3. New York: Wiley.
- Wylie DR, De Zeeuw CI, Simpson JI (1995) Temporal relations of the complex spike activity of Purkinje cell pairs in the vestibulocerebellum of rabbits. *J Neurosci* 15:2875–2887.